Protein composition of the hepatitis A virus quasi-envelope

Kevin L. McKnight[a,b,c], Ling Xie[c,d], Olga González-López[a,b,c], Efraín E. Rivera-Serrano[a,b,c], Xian Chen[c,d], and Stanley M. Lemon[a,b,c,1]

[a]Department of Medicine, University of North Carolina at Chapel Hill, Chapel Hill, NC 27599-7292; [b]Department of Microbiology and Immunology, University of North Carolina at Chapel Hill, Chapel Hill, NC 27599-7292; [c]Lineberger Comprehensive Cancer Center, University of North Carolina at Chapel Hill, Chapel Hill, NC 27599-7295; and [d]Department of Biochemistry and Biophysics, University of North Carolina at Chapel Hill, Chapel Hill, NC 27599-7260

Edited by Mary K. Estes, Baylor College of Medicine, Houston, TX, and approved April 12, 2017 (received for review November 27, 2016)

The *Picornaviridae* are a diverse family of RNA viruses including many pathogens of medical and veterinary importance. Classically considered "nonenveloped," recent studies show that some picornaviruses, notably hepatitis A virus (HAV; genus Hepatovirus) and some members of the Enterovirus genus, are released from cells nonlytically in membranous vesicles. To better understand the biogenesis of quasi-enveloped HAV (eHAV) virions, we conducted a quantitative proteomics analysis of eHAV purified from cell-culture supernatant fluids by isopycnic ultracentrifugation. Amino acid-coded mass tagging (AACT) with stable isotopes followed by tandem mass spectrometry sequencing and AACT quantitation of peptides provided unambiguous identification of proteins associated with eHAV versus unrelated extracellular vesicles with similar buoyant density. Multiple peptides were identified from HAV capsid proteins (53.7% coverage), but none from nonstructural proteins, indicating capsids are packaged as cargo into eHAV vesicles via a highly specific sorting process. Other eHAV-associated proteins ($n = 105$) were significantly enriched for components of the endolysosomal system (>60%, $P < 0.001$) and included many common exosome-associated proteins such as the tetraspanin CD9 and dipeptidyl peptidase 4 (DPP4) along with multiple endosomal sorting complex required for transport III (ESCRT-III)-associated proteins. Immunoprecipitation confirmed that DPP4 is displayed on the surface of eHAV produced in cell culture or present in sera from humans with acute hepatitis A. No LC3-related peptides were identified by mass spectrometry. RNAi depletion studies confirmed that ESCRT-III proteins, particularly CHMP2A, function in eHAV biogenesis. In addition to identifying surface markers of eHAV vesicles, the results support an exosome-like mechanism of eHAV egress involving endosomal budding of HAV capsids into multivesicular bodies.

exosome | multivesicular body | ESCRT | extracellular vesicle | picornavirus

The *Picornaviridae* are a large and diverse family of positive-strand RNA viruses that include numerous pathogens (1). Classically considered "nonenveloped," these viruses package their single-stranded genomes within stable icosahedral protein capsids that are released from cells following cell lysis. However, recent work has revealed that several picornaviruses gain egress from cells in a nonlytic fashion within the lumen of extracellular vesicles shed from the cell. Most notably, hepatitis A virus (HAV; genus Hepatovirus), an important cause of enterically transmitted hepatitis in humans, replicates without cytopathic effect and is released from cells as membrane-wrapped, "quasi-enveloped" (eHAV) virions similar in size and density to exosomes (2). eHAV virions have been identified in sera collected from persons with acute hepatitis A, as well as in supernatant fluids of infected cell cultures. These virions are completely cloaked in host-derived membranes that protect the capsid from neutralizing antibody until the quasi-envelope is degraded within an endosomal compartment (2, 3). Nevertheless, they have specific infectivity similar to naked, nonenveloped HAV particles in cell culture. Coxsackievirus B, poliovirus, and many other members of the genus Enterovirus typically cause lytic infections in cultured cells. However, viruses in this genus are also released within extracellular vesicles before cell lysis, often with many capsids packaged within a single vesicle (4–6). The cellular egress of these classically nonenveloped viruses in membrane-bound vesicles has blurred the distinction between enveloped and nonenveloped viruses and has important implications for pathogenesis (2).

Several lines of evidence indicate that the biogenesis of quasi-enveloped eHAV virions is dependent upon components of the endosomal sorting complex required for transport (ESCRT). For example, the ESCRT-associated protein ALIX (PDCD6IP) interacts with assembled HAV capsids, and RNAi-mediated knockdown of ALIX expression inhibits the release of quasi-enveloped virus from infected cells (2). Although the size and density of eHAV vesicles are consistent with an exosome-like origin in multivesicular bodies (MVBs) (2, 3), eHAV biogenesis remains incompletely defined and the protein composition of the membranes surrounding the quasi-enveloped capsid is unknown. In contrast, the extracellular vesicles involved in egress of enteroviruses have been suggested to be derived from autophagosomes, as they contain lipidated LC3-II, a marker of autophagy, and disrupting autophagy blocks their release (4, 6). However, the protein composition of these extracellular vesicles also has yet to be comprehensively investigated. Thus, for both hepatoviruses and enteroviruses, the cellular mechanisms underlying the biogenesis of membrane-wrapped extracellular virions remain largely obscure and the protein composition of their membranes unknown.

Significance

The nonlytic cellular egress of picornaviruses in extracellular vesicles is likely to be important in disease pathogenesis, but the mechanism(s) underlying this process and the origins of the membranes surrounding virions exiting the cell are poorly understood. We describe a quantitative proteomics analysis of quasi-enveloped hepatitis A virus (eHAV) virions that shows capsids are selected as cargo for vesicular export via a highly specific process, and that infectious eHAV virions possess a host protein complement similar to that of exosomes with CD9 and DPP4 displayed on their surface. eHAV-associated proteins are highly enriched for endolysosomal components and lack markers of autophagy, suggesting an exosome-like mechanism of endosomal sorting complex required for transport-mediated eHAV biogenesis involving endosomal budding that is distinct from the autophagosome-mediated release proposed previously for enteroviruses.

Author contributions: K.L.M., O.G.-L., E.E.R.-S., X.C., and S.M.L. designed research; K.L.M., L.X., O.G.-L., and E.E.R.-S. performed research; K.L.M., L.X., O.G.-L., E.E.R.-S., X.C., and S.M.L. analyzed data; and K.L.M., E.E.R.-S., and S.M.L. wrote the paper.

The authors declare no conflict of interest.

This article is a PNAS Direct Submission.

[1]To whom correspondence should be addressed. Email: smlemon@med.unc.edu.

This article contains supporting information online at www.pnas.org/lookup/suppl/doi:10.1073/pnas.1619519114/-/DCSupplemental.

MICROBIOLOGY

Here we describe the results of a quantitative proteomics study that defines the protein composition of the quasi-enveloped eHAV virion and points to an endosomal, MVB-like origin for these unusual infectious particles.

Results

We adopted a quantitative proteomics approach incorporating metabolic amino acid-coded mass tagging with stable isotopes (AACT; also known as SILAC) (7, 8) to unambiguously distinguish eHAV-associated proteins from proteins present in exosomes similar in size and density to eHAV virions. Supernatant fluids from infected Huh-7.5 human hepatoma cell cultures maintained in [$^{13}C_6$]Lys/[$^{13}C_6$]Arg ("heavy"; H) or [$^{12}C_6$]Lys/[$^{12}C_6$]Arg ("light"; L) media were subjected to low-speed centrifugation at 10,000 × *g* to remove large extracellular vesicles (9). eHAV virions remaining in the medium were concentrated by ultracentrifugation at 100,000 × *g* and then purified by isopycnic equilibrium ultracentrifugation in preformed iodixanol gradients (see *SI Materials and Methods* for details). Fractions containing virus were identified by HAV-specific RT-PCR (Fig. 1*A*) and mixed with fractions of similar density from a gradient loaded in parallel with concentrated supernatant fluids from noninfected cells maintained in the opposing medium. The samples were then subjected to proteolytic digestion, and peptide fragments were identified by liquid chromatography-tandem mass spectrometry (LC-MS/MS) and quantified by AACT (*SI Materials and Methods*). Two independent, reverse AACT labeling experiments were carried out, each with H and L labeling of virus (thus we studied a total of four independent virus samples). In the second experiment, virus and mock-infected supernatant fluid concentrates were mixed before, rather than following, isopycnic ultracentrifugation.

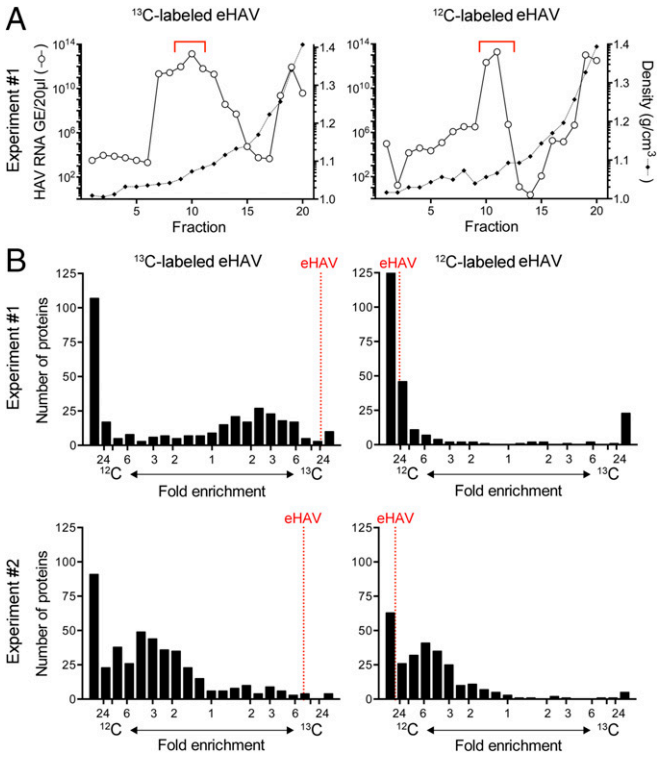

Fig. 1. Stable isotope labeling of eHAV. (*A*) Distribution of HAV RNA (log_{10} scale) in fractions collected from iodixanol gradients loaded with eHAV concentrated from supernatant fluids of infected Huh-7 cell cultures maintained in media containing H [^{13}C] (*Left*) or L [^{12}C] (*Right*) amino acids in experiment 1 and centrifuged to equilibrium. The red brackets indicate fractions that were pooled with fractions of similar density from gradients loaded with supernatant fluids from noninfected cells maintained in the opposing media and subjected to mass spectrometry. ○, HAV RNA; GEs (genome equivalents) per 20 μL; ♦, density (g/cm^3). (*B*) Distribution of isotopic enrichment in peptides identified in a search against the human UniProt database in the four independently ^{13}C-labeled (*Left*) and ^{12}C-labeled (*Right*) eHAV samples submitted for mass spectrometry in experiments 1 (*Top*) and 2 (*Bottom*). In experiment 1, infected and uninfected cell-culture harvests were mixed following density gradient fractionation, whereas these samples were mixed before fractionation in experiment 2. The fold enrichment of HAV-encoded peptides is noted in each panel.

A total of 638 proteins were identified by the presence of at least one unique peptide in at least one of the four samples when screened against the human UniProt database and HAV polyprotein sequence. Of these, 294 were present in both H and L virus samples. Multiple peptides were derived from the four structural proteins of HAV (Fig. S1). One peptide spanned the VP4–VP2 cleavage (QGIFQTVGSGLDHILSLA^DIEEEQMIQSVDR), suggesting that some empty capsids may have been present in the eHAV preparations. Another peptide spanned the VP1pX cleavage site (APLNSNAMLSTES^MMSR) (10), consistent with the lack of VP1pX processing noted previously in eHAV (2). Overall, 53.7% of the sequence of the structural HAV proteins was represented by peptides, whereas no peptides were identified from nonstructural proteins that comprise a larger proportion of the viral polyprotein (Fig. S1). This indicates that the packaging of HAV capsids within the membranes of eHAV vesicles is highly selective, and excludes virally encoded components of the replication complex.

Reflecting robust metabolic labeling, peptides derived from HAV structural proteins were enriched in the H (^{13}C) or L (^{12}C) isotope of their culture medium of origin by 8.4- to 47-fold in the four samples (mean 26.9-fold ± 7.9 SEM) (Fig. 1*B*). However, when all peptides were ranked according to the intensity of H versus L isotope, significant skewing was evident, with a predominance of peptides enriched for L isotope in all four samples (Fig. 1*B* and Table S1): Overall, 42.3% of the peptides were enriched >12-fold for L isotope, versus only 4.6% of peptides for H isotope (P = 0.029 by two-sided Mann–Whitney test). This likely reflects the presence of bovine peptides derived from FCS added to media to maintain cell-culture integrity, as these were not subject to metabolic labeling and thus would be L-enriched. Consistent with this, peptides representing 53% of the identified protein groups shared sequence in common with bovine peptides, rendering their species of origin indeterminate. A total of 292 unique bovine proteins were also identified. These had significantly lower automated H/L ratios than peptides with unique human sequence (P < 0.0001 by ANOVA) or peptides of indeterminate origin (P = 0.0003) (Fig. S2). However, there was no difference between the H/L ratios of peptides of indeterminate versus definitive human origin (P = 0.543), suggesting that most "indeterminate" proteins were actually of human (Huh-7.5 cell) origin.

Peptides representing 105 host proteins (either definitively human or of indeterminate origin) were classified as ≥2-fold–enriched for the cognate eHAV isotope based on automated AACT quantitation of peptides from at least two of the four virus samples (Fig. S3 and Table S1). Peptides from 26 proteins were ≥2-fold–enriched in at least three samples (Fig. 2). The cellular components with which these proteins associate are similar for both sets of proteins (Fig. 3). Over 90% of the proteins in either set have been identified previously in exosomes, and 13 of the 26 proteins identified in at least three virus samples rank among the top 120 exosome-associated proteins in the Vesiclepedia database (www.microvesicles.org) (11). Both sets of proteins were highly enriched for lysosome-associated proteins (P < 0.001), with LAMP1, a classic lysosomal membrane marker, >2-fold–enriched in all four virus samples (geometric mean 8.2-fold).

We focused further on the 26 proteins that were classified as ≥2-fold–enriched in at least three samples (Fig. 2). Whereas 11 were of indeterminate origin, peptide sequences of the

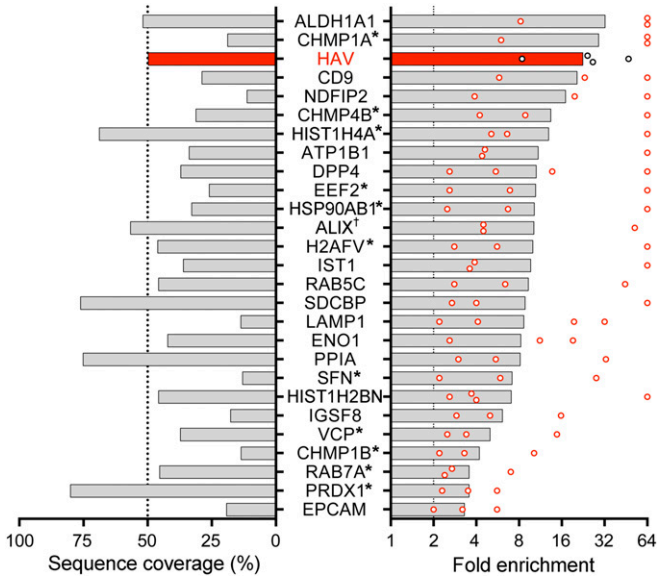

Fig. 2. Sequence coverage and geometric mean fold isotope enrichment of HAV and 26 nonviral proteins with ≥2-fold isotope enrichment (∘) in at least three of four independently labeled eHAV samples submitted for mass spectrometry. *Peptides of indeterminate human versus bovine origin (main text). †ALIX: PDCD6IP.

remaining 15 were uniquely human. Sequence coverage varied from a low of 11.3% (NDFIP2; NEDD4 family-interacting protein 2) to a high of 80.1% (PRDX1; peroxiredoxin 1) (mean 39.7 ± 20.2 SD) (Fig. 2). Five of the 26 proteins are functionally associated with ESCRT-III, including ALIX (also known as PDCD6IP), shown previously to be essential for eHAV biogenesis (2), CHMP1A, CHMP1B, CHMP4B, and IST1, whereas SDCBP (syntenin) plays a key role in syndecan-ALIX–mediated exosome biogenesis (12). Two other proteins, RAB5C and RAB7A, are Rab GTPases that function in endosomal trafficking. Manual inspection of spectra for selected proteins (LAMP1, CHMP1A, CHMP4B, RAB5C, RAB7A, and SDCBP) confirmed quantifiable amounts of peptides and high H/L ratios. This array of proteins and their strong endolysosomal association suggest that eHAV egress involves an MVB-like, endosomal export pathway. Importantly, no peptides derived from the autophagosome membrane marker LC3 were identified in any of the purified virus samples.

Several proteins shown in Fig. 2, including CD9, its binding partner IGSF8 (Ig superfamily member 8), DPP4 (dipeptidyl peptidase 4, CD26), and EPCAM (epithelial cell-adhesion molecule), are expressed on the exterior surface of cell membranes and are thus of interest as proteins potentially displayed on the surface of eHAV vesicles. Manual inspection of the spectra confirmed specific isotopic enrichment of DPP4, CD9, and EPCAM peptides. Interestingly, DPP4 localizes to the apical membrane of polarized hepatic cells (13, 14), whereas our recent work shows that eHAV is secreted across the apical, canalicular membrane of infected *Ifnar1*$^{-/-}$ or *Mavs*$^{-/-}$ mice (14). Apical membrane locations have also been inferred for CD9 and EPCAM in some cell types (15, 16). Proteins expressed exclusively on the apical membrane would not be expected a priori in eHAV vesicles with an endosomal origin. However, DPP4, CD9, and EPCAM have each been identified in exosomes from a variety of cell types (17–19) (Vesiclepedia database), likely reflecting ambiguity in their membrane associations. Indeed, despite its use as a marker of apical membrane polarity, DPP4 is a well-established lysosomal membrane component (20).

We adopted an immunoaffinity approach to physically confirm the association of selected host proteins with eHAV vesicles, quantifying HAV RNA by RT-PCR in virus immunoprecipitated with specific antibodies from gradient fractions containing eHAV. Prior treatment of the eHAV fraction with the detergent Nonidet P-40 resulted in a large (~100-fold) increase in HAV RNA precipitated by an anti-capsid monoclonal antibody (K24F2), consistent with the capsid being occluded by membranes disrupted by the detergent (2) (Fig. 4*A*). Large amounts of virus were also precipitated by antibody to ALIX and DPP4, confirming their association with eHAV. Prior detergent treatment resulted in significant increases in the amount of virus precipitated with anti-ALIX, consistent with previous work suggesting that ALIX interacts with the capsid via two tandem YPX_3L "late domains" in the VP2 capsid protein (2). In contrast, Nonidet P-40 treatment resulted in marked reductions in the amount of viral RNA precipitated by antibody to DPP4, indicating that DPP4 is primarily membrane-associated (Fig. 4*A*). In addition to its dipeptidyl exopeptidase activity, DPP4 has substantial receptor-binding activities, as it interacts with insulin-like growth factor II receptor (IGFIIR) as well as the chemokine receptor CXCR4 (21). Antibody to DPP4 failed to neutralize the infectivity of eHAV virions (Fig. S4), suggesting that this receptor-binding activity is not essential for eHAV entry. Similar negative neutralization results were obtained with antibodies to the tetraspanins CD9, CD63, and CD81 (Fig. S4). Further studies will thus be needed to ascertain how infectious eHAV virions attach to and gain entry into cells.

Next, we determined the ability of an expanded panel of antibodies to precipitate eHAV in the absence of detergent treatment, scoring precipitates relative to the amount of viral RNA pulled down by anti-capsid antibody (K24F2) in the presence of detergent (Fig. 4*B*). Consistently, anti-DPP4 pulled down as much HAV RNA in the absence of detergent as K24F2 did following detergent treatment. Antibodies to CD9, NDFIP2, and histone H4 (HIST1H4A) also precipitated substantial quantities of eHAV, consistent with the exposure of these proteins on the eHAV surface. Lesser amounts of virus (<1%) were precipitated by antibody to LAMP1, or the common exosome components CD63 (isotopically enriched in two virus samples; Table S2) or CD81 (which was present in two of four virus samples but not isotopically enriched) (17). In addition to anti-ALIX, antibodies to several other ESCRT-III–associated proteins not identified in the proteomics screen (CHMP4A, CHMP7, and VPS4B) precipitated large amounts of eHAV

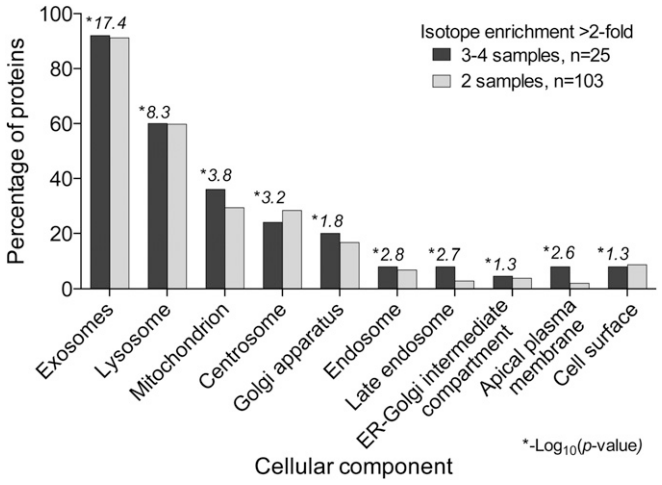

Fig. 3. Cellular components mapped by FunRich (39) to proteins with ≥2-fold isotope enrichment in either ≥2 or ≥3 of 4 independently labeled eHAV samples. *−Log_{10}(*P* value) for enrichment versus UniProt database.

MICROBIOLOGY

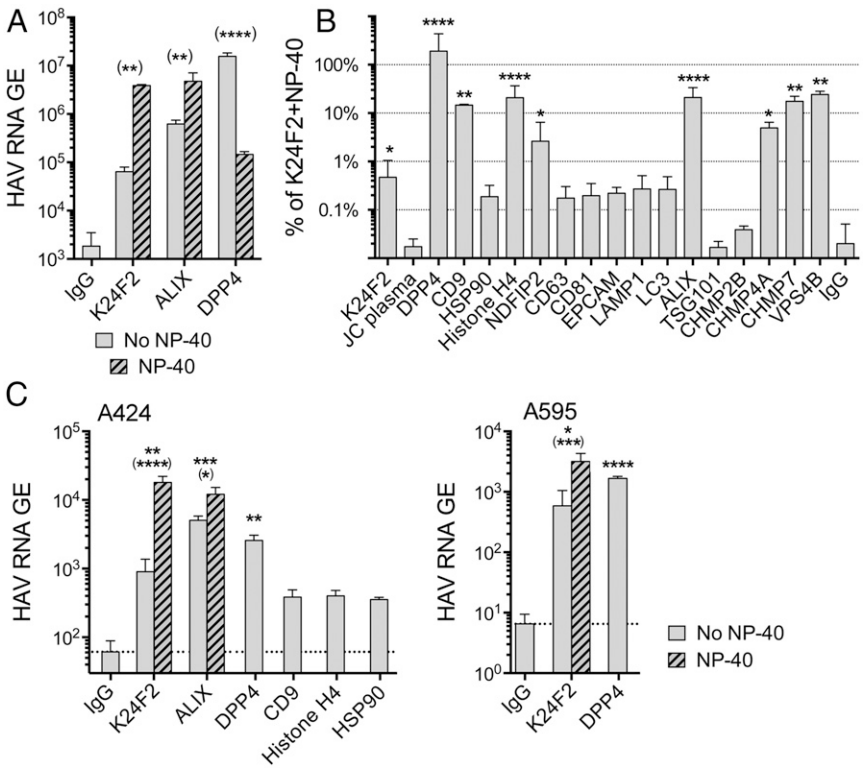

Fig. 4. Immunoprecipitation of eHAV. (*A*) HAV RNA precipitated from gradient-purified eHAV preparations (mean ± SD) by anti-capsid (K24F2), anti-ALIX, or anti-DPP4 antibodies before (solid bars) and after (striped bars) Nonidet P-40 treatment. IgG, nonspecific antibody. (*B*) Antibody-mediated pull-downs of eHAV in the absence of detergent treatment. Results shown are mean percentage ± SD of the amount of HAV RNA precipitated by monoclonal K24F2 anti-HAV following Nonidet P-40 treatment. (*C*) eHAV precipitated by selected antibodies from two acute-phase infection human sera: (*Left*) A424 and (*Right*) A595. IgG, control Ig. $****P < 0.0001$, $***P < 0.001$, $**P < 0.01$, $*P < 0.5$ for comparisons with control IgG by ANOVA with Dunn's or Sidak's tests for multiple comparisons; asterisks in parentheses indicate *P* values for comparisons between Nonidet P-40 treatment and no Nonidet P-40 by unpaired *t* test. $n = 3$ to 9 independent RT-PCR assays.

(Fig. 4*B*). CHMP4A and CHMP4B (which was identified in the screen; Fig. 2) are known to interact with ALIX and CHMP7 (22, 23), and our previous RNAi depletion studies demonstrated that VPS4B is essential for eHAV biogenesis (2). Notably, however, antibody to TSG101, an ESCRT-I–associated protein that unlike ALIX and VPS4B is not required for eHAV biogenesis (2), failed to precipitate eHAV.

To confirm that proteins associated with eHAV produced in cell culture are also present in eHAV in vivo, we immunoprecipitated virus from human serum samples collected from subjects in the earliest stages of acute hepatitis A infection during a nationwide outbreak of the disease in Korea (24). These are rare specimens, and only available in small volumes. Our previous work shows that such sera contain only eHAV without detectable quantities of nonenveloped virus (2). Consistent with this, the ability of anti-capsid antibody to precipitate virus (HAV RNA) from two acute-phase human sera was significantly increased by detergent treatment (Fig. 4*C*). Antibodies to ALIX and DPP4 also precipitated substantial amounts of eHAV from human sera, confirming their presence in eHAV virions in vivo. Lesser amounts of eHAV were precipitated by antibodies to CD9, histone H4, and HSP90.

We assessed the contribution of selected eHAV-associated proteins to biogenesis of quasi-enveloped virions by monitoring the release of eHAV from infected cells transfected with host mRNA-specific siRNA (Table S3). High-grade depletion of ALIX, CHMP2A, CHMP2B, and IST1 mRNAs resulted in significant reductions in the egress of virus into cell-culture supernatant fluids without appreciably affecting the levels of intracellular viral RNA (Fig. 5 and Fig. S5). These results suggest that these ESCRT-III–associated proteins may have essential functions in eHAV biogenesis. Although CHMP1A and CHMP1B knockdowns were much less efficient (Fig. S5*A*), for uncertain reasons partial CHMP1B knockdown reproducibly enhanced eHAV release. Density gradient analysis, a more specific measure of eHAV release than simple supernatant HAV RNA quantitation, confirmed significant reductions in eHAV egress following knockdown of CHMP2A (63% reduction) or combined knockdown of both CHMP2A and CHMP2B (75% reduction) (Fig. 5*B*). Knockdown of CHMP2B alone had substantially less effect (18% reduction), whereas combined CHMP1A and CHMP1B knockdown resulted in a 68% increase in supernatant eHAV. In contrast, high-grade depletion of DPP4 and RAB7A mRNA had no discernible effect on eHAV egress (Fig. 5*A*).

Discussion

Recent studies have brought increasing recognition to the fact that multiple members of the *Picornaviridae* are released from cells enclosed in membranous vesicles in the absence of cell lysis (2–6). This mode of cellular egress has been suggested to play an important role in disease pathogenesis by masking viral antigens from the immune system (2) or increasing the number of viral genomes delivered to single infected cells (6). However, many questions remain concerning the mechanisms underlying the release of virus in extracellular vesicles. Mammalian cells shed a variety of types of extracellular vesicles that are highly heterogeneous in size, density, and protein and nucleic acid composition and differ in their mechanisms of biogenesis (9, 17). The term "exosome" is generally used to describe a specific subset of these extracellular vesicles that are ∼40 to 150 nm in diameter and formed by inward budding of endosomal membranes in an ESCRT-dependent process that results in MVBs containing multiple intraluminal vesicles (hence the alternative term "multivesicular endosomes") (17, 25). MVBs generally transport their cargo to lysosomes for destruction, but some MVBs disgorge their intraluminal vesicles as exosomes following fusion with the plasma membrane. The specific signals controlling this dichotomy of vesicle movement are not well-understood.

We identified proteins associated with eHAV vesicles using a combination of quantitative proteomics and immunoprecipitation with specific antibodies. Importantly, the use of amino acid mass tagging with stable isotopes (7, 8) allowed us to unambiguously identify proteins associated with eHAV versus other extracellular vesicles with size and density equivalent to eHAV in iodixanol

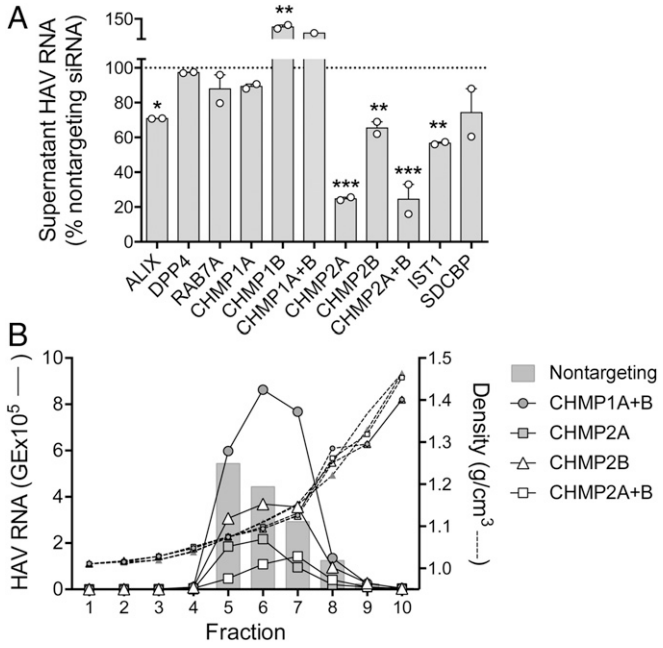

Fig. 5. RNAi analysis of potential DPP4-, RAB7A-, and ESCRT-III–associated host protein function in eHAV biogenesis. (*A*) RT-PCR detection of virus released into supernatant fluids of persistently infected cell cultures between 72 and 96 h after transfection with host mRNA-specific or control, nontargeting siRNA pools. Results represent the percentage HAV RNA relative to that in supernatants from cultures transfected with nontargeting siRNA, and are shown as mean ± range from two independent experiments. $*P < 0.05$, $**P < 0.01$, $***P < 0.001$ by two-way ANOVA with Holm–Sidak's test for multiple comparisons. (*B*) eHAV present in fractions of iodixanol gradients loaded with 96-h supernatants from cell cultures transfected with the indicated host mRNA-specific siRNAs. Nontargeting siRNA control results are shown as bars. Also shown are the density traces (dashed lines) from each gradient. eHAV was quantified by computing the area under the curve (AUC) for peaks in the RNA profiles.

gradients. Over 90% of the proteins that we found to be associated with eHAV have been reported previously in exosomes (Fig. 3) (11). Moreover, eHAV-associated proteins were highly enriched for those that normally localize to the endolysosomal system of cells (Fig. 3). This includes DPP4, which, although an integral apical transmembrane protein, is also associated with lysosomes (20). No array of proteins has been shown to be completely specific for exosomes versus other types of extracellular vesicles formed by outward budding at the plasma membrane rather than inward budding into MVBs (17). Moreover, the protein composition of exosomes may vary with the type of cell from which they are produced. However, the presence of the tetraspanin CD9 and the strong enrichment of endolysosomal proteins in eHAV vesicles are strongly suggestive of an endosomal exosome-like origin for eHAV (9). We also found eHAV to be enriched for RAB5C and RAB7A (Fig. 2), and isoforms of both of these RAB GTPases are known to play prominent roles in endosomal trafficking and exosome biogenesis (12, 26).

Several other conclusions can be drawn from the proteomics data. First, the packaging of HAV capsids into membranous vesicles is not random but instead results from a highly selective and specific sorting process. Despite high peptide coverage for each of the four structural proteins present in the HAV capsid (53.7% overall; Fig. S1), no peptides were identified from the larger, nonstructural segment of the viral polyprotein in any of the four virus samples studied by mass spectrometry. This indicates that nonstructural HAV proteins are not copackaged with capsids in eHAV vesicles, although they are likely present at high local abundance within the cellular compartment(s) in which the viral RNA replicates and the capsid assembles. ALIX–VP2 capsid protein interactions likely play a major role in this sorting process, although other, yet-to-be-determined sorting mechanisms may well be operative (2, 3).

The quantitative proteomics data also point to the engagement of multiple ESCRT-III–associated proteins in eHAV egress. ALIX, CHMP1A, CHMP1B, CHMP4B, and IST1 were all >2-fold–enriched in three of the four virus samples studied by mass spectrometry (Fig. 2), whereas the presence of CHMP4A, CHMP7, and VPS4B was indicated by immunoprecipitation of gradient-purified eHAV with specific antibodies (Fig. 4*A*). The close association of these ESCRT-III–associated proteins with eHAV is consistent with prior studies showing that RNAi-mediated knockdown of either ALIX or VPS4B effectively ablates eHAV release from cells (2). Similar knockdown experiments confirm functional roles for additional ESCRT-III–associated proteins identified in the proteomics screen, including in particular CHMP2A (Fig. 5).

Whereas ESCRT-I and ESCRT-II proteins are important for exosome biogenesis (17, 27), none were associated with eHAV. TSG101, an ESCRT-I–associated protein that is typically present in exosomes derived from MVBs (9), was not isotopically enriched in any of the four eHAV samples subjected to mass spectrometry. Previous RNAi studies also suggest that neither TSG101 nor the ESCRT-0–associated protein HRS is essential for eHAV release (2). Thus, whereas ESCRT-III proteins are required for membrane scission in eHAV biogenesis, there is as yet no evidence that other ESCRTs play a role in eHAV cargo selection. This contrasts with current paradigms for MVB formation and exosome biogenesis (17, 25). HAV may thus usurp only part of, and not the entire, exosome biogenesis pathway to gain egress from infected cells.

Poliovirus and other enteroviruses appear to egress nonlytically from infected cells in autophagosome-derived vesicles containing LC3-II (4, 5, 28). These enteroviral vesicles are much larger than eHAV, and contain a much greater number of viral capsids than eHAV vesicles (2, 6). Their size resembles extracellular vesicles and autophagous blebs shed from the plasma membrane, and is distinct from MVB-derived exosomes that are generally much smaller (<150 nm) and similar to eHAV (2, 17). Nonetheless, it is not possible to fully exclude a role for autophagy-mediated secretion (29, 30) in the biogenesis of quasi-enveloped eHAV vesicles. Purified eHAV preparations contained no detectable peptides derived from LC3, which in its lipidated LC3-II form is associated with autophagosome membranes. However, LC3 appears to be difficult to detect by mass spectrometry in autophagosome-derived extracellular vesicles (31, 32). Nonetheless, eHAV vesicles were not precipitated by anti-LC3 antibody (Fig. 4*B*), and we have shown previously that RNAi-mediated depletion of beclin 1 has no effect on eHAV release (2). Autophagy-related release of poliovirus is inhibited by beclin-1 knockdown (6) but not by spautin 1, an autophagy inhibitor that blocks deubiquitinases targeting beclin 1 (33, 34). Further studies are needed to determine the extent to which eHAV biogenesis may involve beclin 1-independent aspects of secretory autophagy.

Hepatitis E virus, which is phylogenetically distinct from the picornaviruses and classified within its own family, the *Hepeviridae*, and Bluetongue virus, a member of the Orbivirus genus in the *Reoviridae* family, are nonenveloped viruses that also gain egress from cells via nonlytic processes dependent upon ESCRT-associated proteins (reviewed in ref. 3). Unlike HAV, these viruses are dependent upon TSG101 for their egress. We anticipate that additional nonenveloped viruses will be shown to be released nonlytically in extracellular vesicles, and that the responsible mechanisms may prove to be as heterogeneous and varied as the different types of extracellular vesicles released from eukaryotic cells (17).

Materials and Methods

Cells and Plasmids. Huh-7.5 human hepatoma cells (35) and FRhK-4 fetal rhesus kidney cells (36) were cultured in DMEM supplemented with 10% FBS, except as otherwise noted. HM175/p16 virus, a low-passage, noncytopathic, cell culture-adapted variant of the HM175 strain of HAV, has been described previously (37, 38). An infectious molecular clone of its genome, pHM175p16.2 (GenBank accession no. KP879217.1), was assembled, under control of the T7 promoter, from PCR-amplified cDNA fragments using standard methods.

Human Serum Samples. Human serum samples were collected from individuals involved in a nationwide outbreak of hepatitis A in Korea with the approval of the institutional review board of Seoul National University Bundang Hospital (2). Deidentified serum samples were graciously provided by Sook-Hyang Jeong. The UNC Office of Human Research Ethics determined this research did not require Institutional Review Board approval.

Quantitative AACT Proteomics Analysis of Quasi-enveloped eHAV Virions. RNA transcripts were prepared from pHM175p16.2 DNA and transfected into Huh-7.5 cells by electroporation as previously described (2). After culturing for 2 wk in DMEM with 10% FBS, the cells were passaged five times (1:10 split) in media containing [$^{13}C_6$]Lys/[$^{13}C_6$]Arg (H media) or [$^{12}C_6$]Lys/[$^{12}C_6$]Arg (L media) (Thermo Fisher) in parallel with nontransfected cells. Approximately 5×10^6 cells were subcultured in 850-cm^2 roller bottles (Corning) with media supplemented with 25 mM Hepes and exosome-depleted FBS (Thermo Fisher). Roller bottles were placed on an Argos FlexiRoll set at 0.01 rpm in a 35.5 °C incubator with no CO_2. After 5 d, the virus-containing media were removed for storage at 4 °C, the cells were refed, and the roller bottles were cultured for an additional 5 d. Following a second and final collection, media from transfected (infected) and nontransfected (noninfected) cells were clarified by centrifugation twice at 10,000 × *g* for 30 min, thereby removing large extracellular vesicles. eHAV virions remaining in the media were then concentrated by centrifugation at 100,000 × *g* in a Sorvall Ultra 80 ultracentrifuge with a SureSpin 630 rotor (Thermo Scientific) and 36-mL Ultra-Clear tubes (Beckman Coulter). Pellets were resuspended in 100 μL of PBS, layered on top of a preformed preparative iodixanol gradient, and centrifuged to equilibrium as previously described (2). Fractions containing virus were identified by extraction of RNA followed by HAV-specific RT-PCR (2), mixed with fractions of equivalent density from a similar gradient loaded with concentrated supernatant fluids from noninfected cells maintained in the opposing H or L medium, and subjected to either in-gel or in-solution tryptic digestion followed by LC-MS/MS for peptide sequencing and protein identification. Mass spectra were processed and peptides were identified using the Andromeda search engine and MaxQuant software version 1.5.3.2 (Max Planck Institute) against UniProt human and bovine sequence databases and the UniProt HM175/p16 virus polyprotein sequence (A0A0F7Q1W1). The enrichment of proteins with H (^{13}C) or L (^{12}C) isotope was estimated from the H/L ratio of peptides, which was derived from a comparison of the extracted ion chromatogram peak areas of all quantifiable matched light ([^{12}C]-enriched) versus heavy ([^{13}C]-enriched) peptides (7, 8). The cellular components and biological pathways with which these proteins are associated were assessed using open-source FunRich 2.1.2 functional enrichment software and the UniProt and Vesiclepedia databases (11, 39). Complete details are provided in *SI Materials and Methods*.

Statistics. Statistical significance was assessed by ANOVA or unpaired *t* tests as described in *Results*. Calculations were carried out with Prism 6 for Mac OS X software, version 6.0h (GraphPad). A P value <0.05 was considered significant.

ACKNOWLEDGMENTS. The authors thank Dr. Sook-Hyang Jeong, Seoul National University Bundang Hospital, for providing the invaluable acute-phase HAV-infected human serum samples used in this study. This work was supported in part by grants from the National Institutes of Health (R01-AI103083 and U19-AI109965) and University Cancer Research Fund.

1. Ehrenfeld E, Domingo E, Roos RP, eds (2010) *The Picornaviruses* (ASM, Washington, DC).
2. Feng Z, et al. (2013) A pathogenic picornavirus acquires an envelope by hijacking cellular membranes. *Nature* 496:367–371.
3. Feng Z, Hirai-Yuki A, McKnight KL, Lemon SM (2014) Naked viruses that aren't always naked: Quasi-enveloped agents of acute hepatitis. *Annu Rev Virol* 1:539–560.
4. Robinson SM, et al. (2014) Coxsackievirus B exits the host cell in shed microvesicles displaying autophagosomal markers. *PLoS Pathog* 10:e1004045.
5. Bird SW, Maynard ND, Covert MW, Kirkegaard K (2014) Nonlytic viral spread enhanced by autophagy components. *Proc Natl Acad Sci USA* 111:13081–13086.
6. Chen YH, et al. (2015) Phosphatidylserine vesicles enable efficient en bloc transmission of enteroviruses. *Cell* 160:619–630.
7. Chen X, Smith LM, Bradbury EM (2000) Site-specific mass tagging with stable isotopes in proteins for accurate and efficient protein identification. *Anal Chem* 72:1134–1143.
8. Zhu H, Pan S, Gu S, Bradbury EM, Chen X (2002) Amino acid residue specific stable isotope labeling for quantitative proteomics. *Rapid Commun Mass Spectrom* 16:2115–2123.
9. Kowal J, et al. (2016) Proteomic comparison defines novel markers to characterize heterogeneous populations of extracellular vesicle subtypes. *Proc Natl Acad Sci USA* 113:E968–E977.
10. Martin A, et al. (1995) Identification and site-directed mutagenesis of the primary (2A/2B) cleavage site of the hepatitis A virus polyprotein: Functional impact on the infectivity of HAV RNA transcripts. *Virology* 213:213–222.
11. Kalra H, et al. (2012) Vesiclepedia: A compendium for extracellular vesicles with continuous community annotation. *PLoS Biol* 10:e1001450.
12. Baietti MF, et al. (2012) Syndecan-syntenin-ALIX regulates the biogenesis of exosomes. *Nat Cell Biol* 14:677–685.
13. Aït-Slimane T, Galmes R, Trugnan G, Maurice M (2009) Basolateral internalization of GPI-anchored proteins occurs via a clathrin-independent flotillin-dependent pathway in polarized hepatic cells. *Mol Biol Cell* 20:3792–3800.
14. Hirai-Yuki A, Hensley L, Whitmire JK, Lemon SM (2016) Biliary secretion of quasi-enveloped human hepatitis A virus. *MBio* 7:e01998–16.
15. Trzpis M, et al. (2007) Spatial and temporal expression patterns of the epithelial cell adhesion molecule (EpCAM/EGP-2) in developing and adult kidneys. *Nephron Exp Nephrol* 107:e119–e131.
16. The UniProt Consortium (2017) UniProt: The universal protein knowledgebase. *Nucleic Acids Res* 45:D158–D169.
17. Colombo M, Raposo G, Théry C (2014) Biogenesis, secretion, and intercellular interactions of exosomes and other extracellular vesicles. *Annu Rev Cell Dev Biol* 30:255–289.
18. Meckes DG, Jr, et al. (2013) Modulation of B-cell exosome proteins by gamma herpesvirus infection. *Proc Natl Acad Sci USA* 110:E2925–E2933.
19. Tauro BJ, et al. (2012) Comparison of ultracentrifugation, density gradient separation, and immunoaffinity capture methods for isolating human colon cancer cell line LIM1863-derived exosomes. *Methods* 56:293–304.
20. Schröder B, et al. (2007) Integral and associated lysosomal membrane proteins. *Traffic* 8:1676–1686.
21. Metzemaekers M, Van Damme J, Mortier A, Proost P (2016) Regulation of chemokine activity—A focus on the role of dipeptidyl peptidase IV/CD26. *Front Immunol* 7:483.
22. Horii M, et al. (2006) CHMP7, a novel ESCRT-III-related protein, associates with CHMP4b and functions in the endosomal sorting pathway. *Biochem J* 400:23–32.
23. McCullough J, Fisher RD, Whitby FG, Sundquist WI, Hill CP (2008) ALIX-CHMP4 interactions in the human ESCRT pathway. *Proc Natl Acad Sci USA* 105:7687–7691.
24. Jung YM, et al. (2010) Atypical manifestations of hepatitis A infection: A prospective, multicenter study in Korea. *J Med Virol* 82:1318–1326.
25. Hanson PI, Cashikar A (2012) Multivesicular body morphogenesis. *Annu Rev Cell Dev Biol* 28:337–362.
26. Zeigerer A, et al. (2012) Rab5 is necessary for the biogenesis of the endolysosomal system in vivo. *Nature* 485:465–470.
27. Hurley JH (2015) ESCRTs are everywhere. *EMBO J* 34:2398–2407.
28. Jackson WT, et al. (2005) Subversion of cellular autophagosomal machinery by RNA viruses. *PLoS Biol* 3:e156.
29. Ponpuak M, et al. (2015) Secretory autophagy. *Curr Opin Cell Biol* 35:106–116.
30. Zhang M, Kenny SJ, Ge L, Xu K, Schekman R (2015) Translocation of interleukin-1β into a vesicle intermediate in autophagy-mediated secretion. *eLife* 4:e11205.
31. Pallet N, et al. (2013) A comprehensive characterization of membrane vesicles released by autophagic human endothelial cells. *Proteomics* 13:1108–1120.
32. Kimura T, et al. (2017) Dedicated SNAREs and specialized TRIM cargo receptors mediate secretory autophagy. *EMBO J* 36:42–60.
33. Mateo R, et al. (2013) Inhibition of cellular autophagy deranges dengue virion maturation. *J Virol* 87:1312–1321.
34. Liu J, et al. (2011) Beclin1 controls the levels of p53 by regulating the deubiquitination activity of USP10 and USP13. *Cell* 147:223–234.
35. Blight KJ, McKeating JA, Rice CM (2002) Highly permissive cell lines for subgenomic and genomic hepatitis C virus RNA replication. *J Virol* 76:13001–13014.
36. Hopps HE, Bernheim BC, Nisalak A, Tjio JH, Smadel JE (1963) Biologic characteristics of a continuous kidney cell line derived from the African green monkey. *J Immunol* 91:416–424.
37. Jansen RW, Newbold JE, Lemon SM (1988) Complete nucleotide sequence of a cell culture-adapted variant of hepatitis A virus: Comparison with wild-type virus with restricted capacity for in vitro replication. *Virology* 163:299–307.
38. Taylor KL, Murphy PC, Asher LVS, LeDuc JW, Lemon SM (1993) Attenuation phenotype of a cell culture-adapted variant of hepatitis A virus (HM175/p16) in susceptible New World owl monkeys. *J Infect Dis* 168:592–601.
39. Pathan M, et al. (2015) FunRich: An open access standalone functional enrichment and interaction network analysis tool. *Proteomics* 15:2597–2601.